



Biodistribution of Agmatine to Brain and Spinal Cord after Systemic Delivery

 Benjamin M. Clements,  Cristina D. Peterson, Kelley F. Kitto, Lukas D. Caye, George L. Wilcox, and Carolyn A. Fairbanks

Department of Pharmaceutics (B.M.C., C.D.P., C.A.F.), Department of Pharmacology (L.D.C., G.L.W., C.A.F.), Department of Neuroscience (K.F.K., G.L.W., C.A.F.), and Department of Dermatology (G.L.W.), University of Minnesota, Minneapolis, Minnesota

Received July 3, 2023; accepted September 11, 2023

ABSTRACT

Agmatine, an endogenous polyamine, has been shown to reduce chronic pain behaviors in animal models and in patients. This reduction is due to inhibition of the GluN2B subunit of the N-methyl-D-aspartate receptor (NMDAR) in the central nervous system (CNS). The mechanism of action requires central activity, but the extent to which agmatine crosses biologic barriers such as the blood-brain barrier (BBB) and intestinal epithelium is incompletely understood. Determination of agmatine distribution is limited by analytical protocols with low sensitivity and/or inefficient preparation. This study validated a novel bioanalytical protocol using high-performance liquid chromatography tandem mass spectrometry (HPLC-MS/MS) for quantification of agmatine in rat biologic matrices. These protocols were then used to determine the plasma pharmacokinetics of agmatine and the extent of distribution to the CNS. Precision and accuracy of the protocol met US Food and Drug Administration (FDA) standards in surrogate matrix as well as in corrected concentrations in appropriate matrices. The protocol also adequately withstood stability and dilution conditions. Upon application of this protocol to pharmacokinetic study, intravenous agmatine showed a half-life in plasma ranging between

18.9 and 14.9 minutes. Oral administration led to a prolonged plasma half-life (74.4–117 minutes), suggesting flip-flop kinetics, with bioavailability determined to be 29%–35%. Intravenous administration led to a rapid increase in agmatine concentration in brain but a delayed distribution and lower concentrations in spinal cord. However, half-life of agmatine in both tissues is substantially longer than in plasma. These data suggest that agmatine adequately crosses biologic barriers in rat and that brain and spinal cord pharmacokinetics can be functionally distinct.

SIGNIFICANCE STATEMENT

Agmatine has been shown to be an effective nonopioid therapy for chronic pain, a significantly unmet medical necessity. Here, using a novel bioanalytical protocol for quantification of agmatine, we present the plasma pharmacokinetics and the first report of agmatine oral bioavailability as well as variable pharmacokinetics across different central nervous system tissues. These data provide a distributional rationale for the pharmacological effects of agmatine as well as new evidence for kinetic differences between brain and spinal cord.

Introduction

Chronic pain remains a major disability in the United States, affecting 20.4% of the adult population in 2016 and leading to severely decreased quality of life (Dahlhamer et al., 2018; Zelaya et al., 2020). Current pharmacotherapies rely heavily on opioids, which can lead to the development of

hyperalgesia, tolerance, constipation, and in some cases opioid use disorder and respiratory depression (Baldini et al., 2012). Agmatine, an endogenous amine, has been shown to behave as a neurotransmitter as it is synthesized in neurons (Wang et al., 2014), released from nerve terminals in brain and spinal cord after stimulation (Reis and Regunathan, 1998; Goracke-Postle et al., 2006, 2007a), and inactivated by uptake into synaptosomes (Gibson et al., 2002). Furthermore, exogenous administration of agmatine has been shown to reduce chronic pain behaviors (Fairbanks et al., 2000; Courteix et al., 2007; Donertas et al., 2018), opioid tolerance (Kolesnikov et al., 1996), and opioid self-administration (Morgan et al., 2002; Wade et al., 2008; Su et al., 2009). Clinical studies have shown

This work was supported by National Institutes of Health National Institute on Drug Abuse [Grant R01DA035931] (to C.A.F.) and [Grant 5T32DA007234] (to B.M.C.) and the Department of Defense Congressionally Directed Medical Research Program [W81XWH-19-1-0673] (to C.A.F.).

No authors report a conflict of interest with the information presented in this manuscript.

dx.doi.org/10.1124/jpet.123.001828.

ABBREVIATIONS: AUC, area under the curve; BBB, blood-brain barrier; BSA, bovine serum albumin; BSCB, blood-spinal cord barrier; CL, clearance; CNS, central nervous system; F, bioavailability; FDA, US Food and Drug Administration; HPLC-MS/MS, high-performance liquid chromatography tandem mass spectrometry; $K_{p,T}$, tissue-to-plasma concentration ratio at a defined time point; LLOQ, lower limit of quantification; NBD-F, 4-fluoro-7-nitrobenzofurazan; NMDAR, N-methyl-D-aspartate receptor; OCT2, organic cation transporter 2; P-gp, P-glycoprotein; QC, quality control sample; RSD, relative standard of deviation; $t_{1/2}$, terminal half-life; t_{max} , time to reach C_{max} ; ULOQ, upper limit of quantification; V, volume of distribution.

that agmatine can reduce neuropathic pain after oral administration in patients with peripheral neuropathy and lumbar disc-associated radiculopathy (Keynan et al., 2010; Rosenberg et al., 2020). These actions are mediated by the inhibition of the N-methyl-D-aspartate receptor (NMDAR) at the GluN2B subunit by agmatine, which elicits reduced pain behaviors in preclinical models without the side effects seen with nonspecific antagonists (Waataja et al., 2019; Peterson et al., 2021).

In accordance with its proposed central mechanism of action, agmatine is known to cross the blood-brain barrier (BBB) (Piletz et al., 2003). Agmatine is also absorbed from the gastrointestinal tract after oral administration (Molderings et al., 2003). However, these studies quantify agmatine at a singular time point, preventing the determination of total exposure and bioavailability. Changes in agmatine concentration over time in both plasma and central nervous system (CNS) have only been determined after intrathecal administration (Roberts et al., 2005). In this work, the plasma elimination half-life is short (9 minutes in mouse). The CNS elimination, however, is much slower, with a half-life greater than 12 hours in mouse spinal cord. This prolonged exposure in the CNS serves to explain the pronounced reduction in tactile hypersensitivity after injury in mouse seen after intrathecal administration every other day for 8 days (Fairbanks et al., 2000). As the rate of elimination in the spinal cord was determined after intrathecal administration, however, the rate and extent of absorption over time of agmatine from central circulation is incompletely defined. Additionally, the extent of absorption from the gut over time and the absolute oral bioavailability of agmatine is unknown.

Quantification of agmatine after systemic administration has been severely limited by quantification methods. As agmatine is rapidly eliminated and does not distribute readily across biologic barriers via passive diffusion, an analytical method must have a small lower limit of quantification (LLOQ). Without an appropriate LLOQ, quantification is possible in neither plasma at later time points nor tissues with low distribution. Current methods of agmatine quantification are limited by incomplete cleanup for complex biologic matrices, inadequate LLOQ for later time points in plasma, or inefficient chromatographic protocols, preventing larger pharmacokinetic studies (Zhao et al., 2002; Roberts et al., 2005; Dalluge et al., 2015). To refine these methods, we use aspects of the derivatization and chromatographic procedures to develop a novel high-performance liquid chromatography tandem mass spectrometry (HPLC-MS/MS) protocol for agmatine quantification. We then validated this assay in accordance with US Food and Drug Administration (FDA) bioanalytical method standards (<https://www.fda.gov/media/70858/download>). Finally, we performed pharmacokinetic analysis of agmatine after intravenous and oral administration, including determining the distribution to both brain and spinal cord in rat.

Methods and Materials

Chemicals and Reagents. Agmatine sulfate (purity $\geq 97\%$), boric acid, sodium hydroxide, bovine serum albumin, methanol, and 4-fluoro-7-nitrobenzofurazan (NBD-F) were purchased from MilliporeSigma (St. Louis, MO). $^{13}\text{C}_4$ -agmatine sulfate was synthesized by Cambridge Isotope Laboratories (purity $\geq 98\%$) (Tewksbury, MA). Ethyl acetate was purchased from Honeywell (Charlotte, NC). Liquid chromatography-mass spectrometry (LC-MS)-grade water, acetonitrile, isopropanol,

and formic acid were purchased from Fisher Scientific (Waltham, MA). Blank pooled rat plasma was purchased from Innovative Research, Inc. (Novi, MI).

Animals. For plasma pharmacokinetic studies, Sprague-Dawley rats of both sexes with surgically implanted indwelling jugular catheters (Envigo, Indianapolis, IN) were used (200–400 g). For CNS distribution studies, Sprague-Dawley rats of both sexes (Envigo) were used (200–300 g). Rats were socially housed with two animals per cage and maintained on a 12-hour light/dark cycle with access to food and water ad libitum. All experiments were performed within the light phase of the cycle. Rats were housed in the Research Animal Resources facility in the Academic Health Center of the University of Minnesota. Protocols for all animal experiments received approval by the University of Minnesota Institutional Animal Care and Use Committee and were performed in accordance with the *Guide for the Care and Use of Laboratory Animals*.

Preparation of Calibration and Quality Control Standards. Compounds undergoing analysis were initially dissolved in dimethyl sulfoxide (DMSO) to create a 1-mg/ml stock solution. This solution was then aliquoted and diluted in methanol to generate stock solutions at 1000, 100, 10, and 1 ng/ml (internal standard solutions were made at 1000 ng/ml only). Appropriate volumes of each of these stocks were taken to generate various concentrations when dried and finally diluted to 100 μl , forming the calibration curve and quality control standards. Stock solutions were stored at -20°C between uses.

Sample Preparation. Agmatine matrix was prepared by dissolving 5% bovine serum albumin (BSA) (w/v) in phosphate-buffered saline (pH = 7.5). CNS homogenate was generated by sonication on ice of brain in 5% BSA in PBS (w/v).

For agmatine analysis, calibration stock or quality control stock was added to microcentrifuge tubes alongside isotopically labeled $^{13}\text{C}_4$ -agmatine sulfate as an internal standard and dried under nitrogen. One hundred microliters of matrix was added to the tubes, which then underwent protein precipitation. Briefly, 200 μl of ice-cold isopropanol was added to each tube to precipitate soluble protein. Each tube was vortexed at 1500 rpm for 10 minutes and centrifuged at 16.1 g for 10 minutes to remove precipitated protein. Two hundred fifty microliters of supernatant was collected and added to Amicon MC-GV 0.22- μm centrifuge filters (Millipore), which were centrifuged at 16.1 g for 20 minutes. Filtrate was dried completely under vacuum. After protein precipitation, agmatine was derivatized with NBD-F. One hundred microliters of borate buffer (pH 9.5) was added to each tube, which was vortexed at 1500 rpm for 10 minutes. To each tube 60 μl of NBD-F solution in acetonitrile (10 mM) was added, and the tubes were briefly vortexed for 10 seconds and placed on a heating block at 60°C for 10 minutes. Within 2 minutes of removal from the heating block, the reaction was ended by addition of ice-cold 40 μl of 0.3% formic acid in water and placement of samples on ice. After 30 minutes on ice, samples underwent liquid-liquid extraction. One milliliter of ethyl acetate was added, and samples were vortexed at 1500 rpm for 10 minutes and centrifuged at 16.1 g for 10 minutes. Nine hundred microliters of organic phase was added to a clean tube and completely dried under nitrogen. NBD-F-agmatine was then reconstituted in mobile phase (97% H_2O , 3% acetonitrile, 0.1% formic acid).

Instrumentation. Analysis was performed using reverse-phase liquid chromatography on an Agilent 1200 Series HPLC coupled to a TSQ Quantum Classic mass spectrometer in positive ion mode. The method used a Waters ACQUITY UPLC HSS T3 column (1.8 μm , 2.1×50 mm), which was held at 35°C during separation. These instruments belonged to and were maintained by the Clinical Pharmacology Analytical Services Laboratory of the College of Pharmacy of the University of Minnesota.

For agmatine, a gradient elution with an aqueous mobile phase (deionized water with 0.1% formic acid) and an organic mobile phase (acetonitrile with 0.1% formic acid) was used as follows: starting at 97% aqueous and 3% organic, the proportion of organic phase was increased to 48% linearly over 2 minutes (0 minutes \rightarrow 2 minutes). This ratio of 52% aqueous and 48% organic was held

for 1 minute (2 minutes → 3 minutes), after which the proportion of organic phase was increased to 97% over 2 minutes (3 minutes → 5 minutes). The 3% aqueous and 97% organic ratio was held for 0.5 minutes (5 minutes → 5.5 minutes). For an additional 30 seconds, the ratio was linearly returned to the starting proportion of 97% aqueous and 3% organic (5.5 minutes → 6 minutes), which was held until the end of the runtime of 10 minutes (6 minutes → 10 minutes). A gradient elution was used to expedite analysis by reducing assay length as opposed to isocratic methods. Columns were reequilibrated for 1 minute between each analysis with 97% aqueous and 3% organic phases.

The mass-to-charge (m/z) transitions and collision voltages (V) were as follows: agmatine 294.2 → 235 (20) and $^{13}\text{C}_4$ -agmatine 298.2 → 239 (20).

Method Validation. Bioanalytical method validations were performed in accordance with the FDA bioanalytical method validation guidelines (<https://www.fda.gov/media/70858/download>).

Calibration curves consisted of a minimum of 13 standards between the lower limit of quantification (LLOQ) and upper limit of quantification (ULOQ). LLOQ was defined as the lowest concentration that produced a signal-to-noise ratio $\geq 20:1$, with accuracy and precision within a limit of 20%. Quality control concentrations and ULOQ were kept within accuracy and precision of 15%. Carryover between samples was deemed acceptable if, after analysis of the ULOQ, blank response was below 20% of the LLOQ.

Precision and accuracy of the methods were determined by calculating the percent relative standard deviation (% RSD) and percent bias (% Bias), respectively. Quality controls were prepared with parallel samples per concentration, comparing among five samples for both precision and accuracy, and analyzed both within and between days, covering 3 days.

As endogenous agmatine limits accurate quantification using blank plasma or CNS, 5% BSA was used as a substitute matrix for these matrices. To assess the adequacy of the substitute matrix, accuracy and precision were tested in blank plasma and CNS by calculating concentration of solutions with known agmatine mass added, corrected for determined endogenous concentration in pooled plasma or CNS and recovery determined.

Stability was assessed by comparing freshly prepared samples to samples from environments appropriate to potential experimental conditions. Long-term stability was tested by storing set concentrations in matrix at -80°C for 28 days. Freeze-thaw stability was tested by storing at -80°C in matrix, bringing to room temperature, and re-freezing thrice prior to analysis. Stability of processed samples was tested by storing at 4°C for 3 days or room temperature for 24 hours.

Dilution integrity was assessed by determining accuracy and precision of quantification using % RSD and % Bias, respectively. For agmatine, 50,000- and 5000-ng/ml working solutions were diluted at a ratio of 1:100 and 1:10, respectively, to a final concentration of 500 ng/ml. This concentration was chosen as it falls within the analytical range. For each dilution, precision and accuracy were determined by comparing five independent samples.

Application to Pharmacokinetic Studies in Rat. For plasma pharmacokinetics studies, agmatine solutions were administered either intravenously via jugular catheter or orally via oral gavage. Dosing solutions for intravenous administration were prepared by dissolving agmatine sulfate to appropriate concentration in vehicle to provide the appropriate dose at 1 ml/kg administration volume in 0.9% sterile-filtered saline. The jugular vein was accessed via indwelling catheter. Drug solution delivery and blood samples extraction were completed by connection of the catheter and syringe using PinPort injectors (Instech, Philadelphia, PA) to provide aseptic repeat access. At assigned time points, 200 μl of blood was drawn, with a maximum of six extractions per 24 hours. From this blood 100 μl of plasma was obtained. After each intravenous bolus and blood draw, 200 μl of 0.9% sterile saline was used to flush the catheter, which was then locked using 110 μl of 500 units/ml heparin: glycerol. For 3 and 30 mg/kg agmatine sulfate, 10 and 9 rats were used, respectively.

For oral administration, agmatine sulfate was dissolved to the appropriate concentration in water to provide the appropriate dose at 1 ml/kg administration volume. Oral gavage was performed by restraining the rat by placing the index and middle fingers along the side of the head, with the other fingers holding the torso around the rib cage, keeping the catheter port in between the middle and index fingers to prevent damage. Drug solution was given by placement of a gavage needle (20G \times 38 mm) in the esophagus and rapid administration. Blood draw was performed in accordance with intravenous pharmacokinetic studies. For 100 and 300 mg/kg agmatine sulfate, six and eight rats were used, respectively.

For agmatine CNS distribution studies, agmatine was administered intravenously via tail vein injection at 100 mg/kg in 0.9% sterile-filtered saline. At predetermined time points between 15 minutes and 12 hours, animals were sacrificed via isoflurane overdose and decapitated ($n = 6$ per time point). Trunk blood was collected in heparinized tubes, obtaining an estimated 1 ml to obtain a minimum of 300 μl plasma. Brain was extracted manually, and spinal cord was extracted using hydraulic extrusion as described previously (Roberts et al., 2005). Briefly, after decapitation, the caudal end of the spinal column was exposed, and a blunt-tipped needle filled with 0.9% sterile-filtered saline was inserted. The plunger was depressed to place pressure on the spinal cord, which is extruded intact from the rostral end of the column. Brain was isolated via gross dissection. The brain and spinal cord were heat stabilized using a Stabilizer system (Denator AB, Uppsala Park, Sweden) to prevent endogenous metabolism of agmatine in extracted CNS tissues.

After collection, blood was immediately placed in heparinized tubes (Greiner Bio-One). Plasma was separated by centrifugation at 5 g for 10 minutes at 4°C . Plasma, heat-treated brain, and heat-treated spinal cord were stored at -80°C until analyzed via HPLC-MS/MS. Prior to analysis, brain and spinal cord were homogenized via sonication in 2 \times (w/v) 5% BSA and stored at -80°C until analysis.

Data Analysis. Plasma, brain, and spinal cord concentration-time profiles were analyzed using Phoenix WinNonlin version 8.3 (Certara USA Inc., Princeton, NJ). Pharmacokinetic parameters were determined using noncompartmental analysis. Areas under the curve (AUCs) for concentration-time profiles were determined by linear trapezoidal integration, with AUC to the last time point (AUC_{Last}) calculated directly from the concentration-time profile, and AUC to infinity ($\text{AUC}_{0-\infty}$) was extrapolated from the final time point to infinity by dividing the final time point by the terminal elimination rate constant (λ_z).

Clearance (CL/F), terminal half-life ($t_{1/2}$), and volume of distribution (V/F) for plasma kinetics were calculated using noncompartmental analysis by the following equations, respectively:

$$\text{CL/F} = \frac{\text{Dose}}{\text{AUC}_{0-\infty}} \quad (1)$$

$$t_{1/2} = \ln(2)/\lambda_z \quad (2)$$

$$\text{V/F} = \frac{\text{Dose}}{\text{AUC}_{0-\infty} * \lambda_z} \quad (3)$$

Additionally, terminal half-life was determined for brain and spinal cord using eq. 2. For intravenous delivery, clearance and volume of distribution are reported as CL and V, respectively, as bioavailability (F) is considered to be equal to 1.

The brain-plasma and spinal cord-plasma partition coefficients ($K_{P,\text{Brain}}$ and $K_{P,\text{Spinal Cord}}$) were calculated as a ratio of AUCs of concentration-time profiles as defined in eqs. 4 and 5, respectively:

$$K_{P,\text{Brain}} = \frac{\text{AUC}_{0-\infty,\text{Brain}}}{\text{AUC}_{0-\infty,\text{Plasma}}} \quad (4)$$

$$K_{P, \text{Spinal Cord}} = \frac{AUC_{0-\infty, \text{Spinal Cord}}}{AUC_{0-\infty, \text{Plasma}}} \quad (5)$$

To assess the extent of distribution over time, eq. 6 describes the tissue-to-plasma concentration ratio at time *t* ($K_{P,t}$):

$$K_{P,t} = \frac{\text{Concentration}_{\text{Tissue}}}{\text{Concentration}_{\text{Plasma}}} \quad (6)$$

Sex differences were tested using Student's *t* test. All graphical representation and statistical analysis were done in GraphPad Prism 7 (GraphPad Software, La Jolla, CA). Data are presented as mean ± S.E.M. when applicable. Sample numbers are reported in figure legends.

Results

Agmatine Detection and Quantitative Method Validation. All quantification of agmatine was performed using an Agilent 1200 Series HPLC coupled to a TSQ Quantum Classic mass spectrometer in positive ion mode. The HPLC-MS/MS protocol was successfully validated for linearity, accuracy, precision, stability, and dilution integrity.

Standard curves were modeled using linear regression with a 1/*x* weighting factor. Owing to the endogenous nature of agmatine, a surrogate matrix of 5% BSA was used for generation of standard curves and quality control samples (QCs) to accurately quantify total concentration in both plasma and CNS tissues. To determine selectivity in this surrogate matrix, the signal-to-noise ratios of the LLOQ sample and blank matrix (5% BSA in PBS) were compared. A minimum difference of 5 times signal was considered adequately sensitive, which was achieved. Representative spectra are shown in Fig. 1.

Accuracy and precision were determined by assessing five sets of QCs in 5% BSA over 3 days. All QCs, including LLOQ (5 ng/ml) and ULOQ (1000 ng/ml), were within acceptable limits of ±15% of nominal concentration or ±20% for LLOQ (Table 1). To confirm the validity of the use of 5% BSA as a surrogate matrix, pooled rat plasma and rat CNS homogenate were spiked with known concentrations of agmatine and final concentrations were quantified. These final concentrations were corrected for calculated endogenous levels, and accuracy, precision, and recovery were determined. At all concentrations in both matrices, the validation criteria were met (Table 2). The final analytical range was defined at 5–1000 ng/ml. Carryover between samples was within appropriate ranges, with less than 20% of LLOQ in blank mobile phase after a run of ULOQ and less than 5% of internal standard (data not shown).

Stability of agmatine was assessed in the conditions expected to occur during storage and sample preparation (Table 3). Agmatine was stable in 5% BSA at –80°C for 28 days, with or without three freeze-thaw cycles. Additionally, after derivatization by NBD-F, agmatine was stable at 4°C for 3 days and at room temperature for 24 hours.

As pharmacokinetic studies show concentrations in plasma beyond the analytical range, the dilution integrity of agmatine in pooled rat plasma was tested. A known concentration of 500 ng/ml in 5% BSA was diluted by one (1:10) or two (1:100) orders of magnitude. Precision and accuracy at both dilution factors were within the validation criteria of ±15% (Table 4).

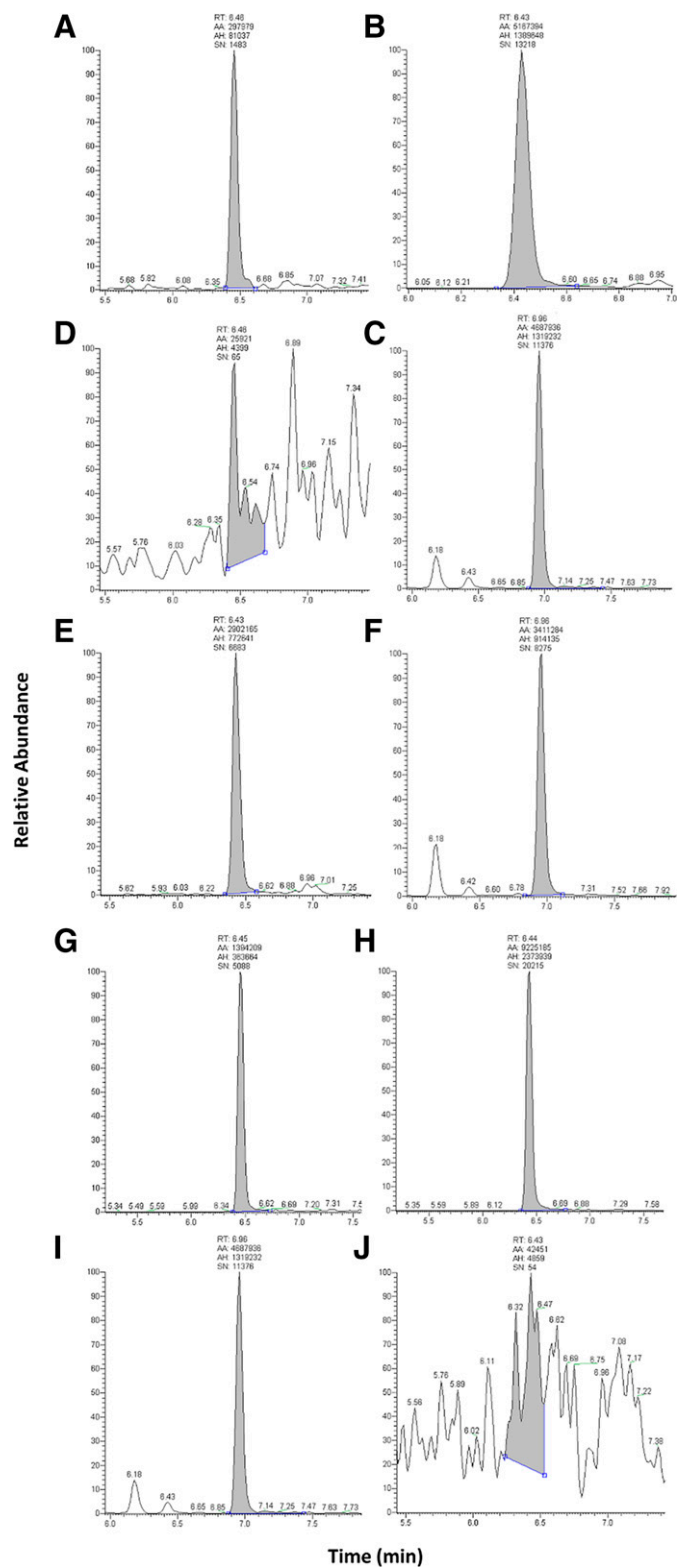


Fig. 1. Chromatograms of agmatine and ¹³C₄-agmatine in various matrices. Peaks of (A) agmatine at LLOQ (5 ng/ml) in 5% BSA; (B) agmatine at LLOQ in rat plasma; (C) agmatine at LLOQ in rat CNS homogenate; (D) blank 5% BSA; (E) blank rat plasma; (F) blank rat CNS homogenate; (G) ¹³C₄-agmatine in 5% BSA; (H) ¹³C₄-agmatine in rat plasma; (I) ¹³C₄-agmatine in rat CNS homogenate; and (J) blank mobile phase (97% H₂O, 3% acetonitrile, 0.1% formic acid). AA, automatic area; AH, automatic height; RT, retention time; SN, signal to noise.

TABLE 1
Intra- and interday precision and accuracy of agmatine analytical method in 5% BSA

Concentration (ng/ml)	% BSA in PBS					
	Intraday			Interday		
	Measured Concentration (Mean \pm S.D.; ng/ml)	Precision (% RSD)	Accuracy (% Bias)	Measured Concentration (Mean \pm S.D.; ng/ml)	Precision (% RSD)	Accuracy (% Bias)
5	5.15 \pm 0.40	7.81	3.08	4.78 \pm 0.69	14.5	-4.48
8	8.26 \pm 0.23	2.73	3.27	8.33 \pm 1.02	12.2	4.11
80	78.3 \pm 0.97	1.23	-2.18	79.3 \pm 1.67	2.10	-0.83
800	785 \pm 14.7	1.87	-1.84	789 \pm 23.9	3.03	-1.33
1000	967 \pm 15.6	1.62	-3.34	980 \pm 33.9	3.46	-2.05

Plasma Pharmacokinetics of Agmatine after Intravenous and Oral Administration. After validation of the bioanalytical method for agmatine quantification, the HPLC-MS/MS protocol was applied to pharmacokinetic studies in rats after both intravenous and oral administration. Catheterized Sprague-Dawley rats received intravenous or oral agmatine, and blood was taken serially at preassigned time points, allowing determination of individual pharmacokinetic parameters for each animal. Intravenous agmatine exhibited a biexponential decline after both doses tested, with all time points assessed above the lower limit of quantification (Fig. 2A). The elimination half-life was comparable between doses (18.9 \pm 1.25 minutes at 3 mg/kg, 14.9 \pm 1.84 minutes at 30 mg/kg), as was seen with clearance and volume of distribution (Table 5).

Oral agmatine showed an initial absorption phase followed by a biphasic decline in plasma (Fig. 2B). The $t_{1/2}$ was greater after oral administration of 300 mg/kg than after intravenous administration, although 100 mg/kg oral lacked a significant difference from the elimination half-lives of both intravenous doses (Table 5). Furthermore, oral bioavailability for agmatine was calculated as 29.0% and 35.0% at 100 and 300 mg/kg, respectively.

CNS Distribution and Pharmacokinetics. Previous studies have assessed agmatine distribution to the CNS from the systemic circulation, but the extent of exposure over a time course consistent with the pharmacological duration of action of systemically administered agmatine has not been fully characterized. Therefore, after intravenous administration of agmatine, concentrations in plasma and brain were measured over time using the developed HPLC-MS/MS methods. Concentration-time profiles in plasma, spinal cord, and brain were generated from 15 to 720 minutes (Fig. 3A). To compare with endogenous levels, tissues from rats naive to exogenous agmatine were collected and analyzed. Plasma levels of agmatine exhibited a biexponential decline. Distribution to

the brain was rapid, with time to reach C_{max} (t_{max}) occurring at 15 minutes, but distribution to the spinal cord was delayed (t_{max} = 120 minutes). Concentration in spinal cord tissue was lower than brain at time points between administration and spinal cord t_{max} (15–60 minutes). In addition, concentrations were lower in spinal cord than brain at all further time points, although only significant at 240 minutes.

Compared with serial sampling studies (Fig. 2A), elimination half-life in terminal sampling studies was extended (104 minutes), allowing for detection at 12 hours postdose (Table 6). This distinction between both studies is further shown by an increased volume of distribution and a decreased clearance. Even with this slowed decline, elimination half-life in CNS tissues was greater than in plasma, between 8.5 (brain) and 14.3 (spinal cord) hours. The tissue-to-plasma concentration ratio at a defined time point ($K_{P,T}$) represents differences in distribution between systemic circulation and the CNS. Endogenous agmatine levels are generally greater within the CNS compared with plasma, generating an initial $K_{P,T}$ greater than one, which quickly drops upon exogenous agmatine administration as plasma concentration increases (Fig. 3B). As the rate of elimination is slow in CNS, the $K_{P,T}$ continues to increase over time, surpassing 1 over 240 minutes. Similar to the differences in tissue concentrations, tissue-to-plasma ratio in spinal cord is lower than in brain at all time points after agmatine administration, with significance at all time points except 720 minutes. To interpret the extent of distribution over the entire time course assessed, the $AUC_{0-\infty}$ of plasma and CNS tissues were compared (Table 6). These K_P values were below one for all tissues.

Sex Difference Analysis. To meet contemporary standards of scientific rigor as well as to account for known differences in clinical representations of pain (Osborne and Davis, 2022), animal sex was assessed as a biologic variable in all applicable studies. All studies directly compared both concentrations and individual pharmacokinetic parameters

TABLE 2
Precision and accuracy of agmatine analytical method in plasma and CNS

Concentration (ng/ml)	Plasma				CNS			
	Corrected Measured Concentration (Mean \pm S.D.; ng/ml)	Recovery (%)	Precision (% RSD)	Accuracy (% Bias)	Corrected Measured Concentration (Mean \pm S.D.; ng/ml)	Recovery (%)	Precision (% RSD)	Accuracy (% Bias)
5	4.28 \pm 0.66	85.6 \pm 13.2	15.5	-14.5	5.51 \pm 0.27	85.6 \pm 13.2	4.87	10.24
8	9.00 \pm 0.29	113 \pm 36.3	3.23	12.6	8.44 \pm 0.96	113 \pm 36.3	11.4	5.54
80	84.9 \pm 0.19	106 \pm 0.24	0.23	6.18	79.5 \pm 2.24	106 \pm 0.24	2.81	-0.68
800	815 \pm 0.06	102 \pm 0.01	0.01	1.87	764 \pm 22.6	102 \pm 0.01	2.95	-4.48
1000	1047 \pm 0.03	105 \pm 0.00	0.00	4.68	993 \pm 22.8	105 \pm 0.00	2.30	-0.71

TABLE 3
Stability of agmatine in 5% BSA under various conditions

Stability Conditions	Concentration (ng/ml)		% RSD	% Bias
	Predicted	Actual		
Room temperature (24 hours)	8	8.57 ± 0.95	11.1	7.10
	80	88.1 ± 2.31	2.63	10.1
	800	843 ± 20.9	2.48	5.41
4°C (3 days)	8	7.46 ± 0.90	12.1	-6.74
	80	84.7 ± 3.28	3.88	5.92
	800	795 ± 15.5	1.95	-0.65
Long-term stability (-80°C for 28 days)	8	8.44 ± 0.86	10.2	5.54
	80	79.5 ± 2.00	2.52	-0.68
	800	794 ± 20.2	2.64	-4.48
Freeze-thaw (3 cycles)	8	7.93 ± 0.54	6.82	-0.87
	80	78.2 ± 1.31	1.67	-2.24
	800	781 ± 16.6	2.12	-2.39

of males relative to females using Student's *t* test. In catheterized animals, both doses of intravenous agmatine and one dose of oral agmatine showed a sex difference in plasma agmatine concentration at one time point, but these differences were not consistent within the studies nor were any differences seen in average pharmacokinetic parameters. In terminal studies, female rats exhibited greater plasma and brain agmatine concentrations at 60 minutes, but this difference was not present at any other time points. Of note, naïve plasma agmatine concentrations were higher in female rats. This difference may be representative of known sex differences in polyamine synthetic pathways (Feroli et al., 1999; Barron et al., 2008), although the significance was not seen in other studies in our laboratory that included naïve samples (data not shown).

Discussion

Agmatine has been extensively shown to reduce chronic pain behaviors (Horváth et al., 1999; Fairbanks et al., 2000; Courteix et al., 2007; Donertas et al., 2018; Rosenberg et al., 2020) and opioid self-administration in preclinical models (Morgan et al., 2002; Wade et al., 2008; Su et al., 2009). As these actions of agmatine are believed to occur via the NMDAR within the CNS (Waataja et al., 2019; Peterson et al., 2021), central availability of the drug is required after systemic delivery. Agmatine has been confirmed to cross the BBB (Piletz et al., 2003) and be orally bioavailable (Molderings et al., 2003), although the extent to which these processes occur is incompletely understood. Limits to this understanding are due in part to difficulty in agmatine quantification in

TABLE 4
Dilution integrity of agmatine in 5% BSA

	Dilution Factor	Concentration (ng/ml)		% RSD	% Bias
		Predicted	Actual		
Agmatine (plasma)	1:10	500	467 ± 6.37	1.37	-5.88
	1:100	500	479 ± 22.3	4.64	-4.73

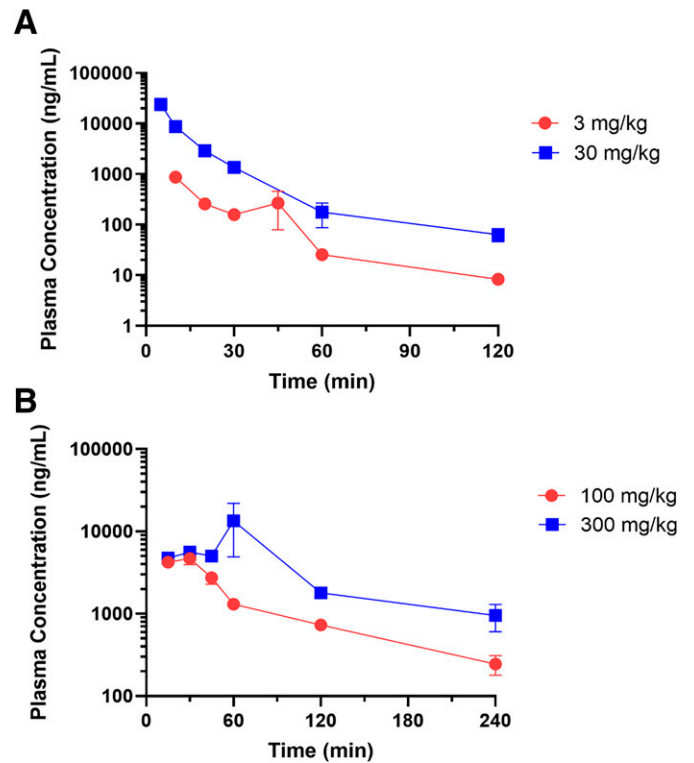


Fig. 2. Plasma pharmacokinetics of agmatine after intravenous and oral administration in Sprague-Dawley rat. (A) Plasma concentration-time profiles after a single i.v. dose via jugular catheter of 3 or 30 mg/kg agmatine sulfate in Sprague-Dawley rat ($n = 10$ and 9 , respectively). (B) Plasma concentration-time profiles after a single oral dose via oral gavage of 100 or 300 mg/kg agmatine sulfate in Sprague-Dawley rat ($n = 6$ and 8 , respectively). Data are presented as mean \pm S.E.M.

complex biologic matrices. Previous methods, although effective in their contexts, led to incomplete sample cleanup and/or inadequate lower limits of quantification for determination of plasma and CNS concentration-time profiles (Zhao et al., 2002; Roberts et al., 2005; Dalluge et al., 2015). Therefore, we developed a novel HPLC-MS/MS protocol for quantification of agmatine in rat plasma, spinal cord, and brain, which we then applied to determine the plasma pharmacokinetics, oral bioavailability, and CNS distribution of agmatine in rat. The sensitivity, linearity, carryover, accuracy, precision, and stability of agmatine in matrix were within FDA-described ranges at all concentrations defined (<https://www.fda.gov/media/70858/download>). Due to the endogenous presence of agmatine in plasma and CNS, the method could not use blank tissue as a matrix for validation or quantification. Therefore, 5% BSA in saline was used as a surrogate matrix. The quantification of agmatine in plasma and CNS using this surrogate matrix was shown to be accurate and precise, supporting its use in the pharmacokinetic studies. Adequate detection required protein precipitation prior to derivatization using NBD-F, but as reagents involved in derivatization are not compatible with the HPLC-MS/MS system, an additional liquid-liquid extraction step was required. Due to this additional step and the derivatization requirement, extraction efficiency and matrix effects were not able to be determined. Nonetheless, accuracy and precision of quantification were confirmed, supporting the use of this assay.

Using these validated bioanalytical methods, the systemic pharmacokinetics of agmatine were assessed via serial sampling

TABLE 5

Summary of pharmacokinetic parameters of agmatine after intravenous and oral administration

Summary of pharmacokinetics parameters of agmatine after intravenous or oral administration in Sprague-Dawley rat. An ordinary one-way ANOVA with Tukey's multiple comparison test was performed comparing $t_{1/2}$ between doses and administration type. Results are presented as mean or mean \pm S.E.M.

	Intravenous		Oral	
Dose (mg/kg)	3	30	100	300
$t_{1/2}$ (min)	18.9 \pm 1.25	14.9 \pm 1.84	74.4 \pm 11.1	117 \pm 32.8 ^{a,b}
C_{max} (ng/ml)	335 \pm 130	23,930 \pm 825	4730 \pm 563	14,494 \pm 7806
t_{max} (min)	10	5	23.6 \pm 2.81	45 \pm 4.59
AUC _{0-∞} (ng/ml/min)	35,075 \pm 4510	421,956 \pm 21,095	336,452 \pm 34,544	122,2925 \pm 347,552
CL (ml/min/kg)	98.6 \pm 10.7	72.4 \pm 3.29	—	—
CL/F (ml/min/kg)	—	—	317 \pm 32.2	375 \pm 179
V (l/kg)	2.66 \pm 0.296	1.507 \pm 0.135	—	—
V/F (l/kg)	—	—	32.2 \pm 3.33	52.1 \pm 13.8
F (%)	—	—	29.0	35.0

Dashes represent pharmacokinetic parameters not applicable to the defined treatment condition.

^a $P < 0.05$ from intravenous low dose.

^b $P < 0.05$ from intravenous high dose.

after administration. After intravenous administration in rat, agmatine exhibited a distributional phase followed by an elimination phase, as supported by previous kinetics performed in mice (Roberts et al., 2005). No dose dependence in intravenous pharmacokinetics was observed, with the elimination half-life values determined to be within 15 and 20 minutes. These values are greater than the half-lives previously reported in plasma (Raasch et al., 2002; Nguyen et al., 2003; Piletz et al., 2003; Roberts et al., 2005). This variability is likely due to differences both between mice and rats and between rat strains.

In addition, the HPLC-UV/Vis (UV-visible spectroscopy) protocols used may have sensitivity limits preventing accurate quantification at later time points. This inability to detect at later time points may also drive the monoexponential decline seen in these previous studies compared with the biexponential decline replicated here.

After oral administration of agmatine at 100 and 300 mg/kg, bioavailability in rat is 29% and 35%, respectively. Previous reports have demonstrated oral absorption of agmatine as well as BBB penetration of orally administered agmatine (Molderings et al., 2003; Bergin et al., 2019). However, these studies did not interpret the extent of absorption over time, preventing complete quantification of oral bioavailability. As seen after intravenous administration, agmatine exhibits biphasic decline but with a much greater elimination half-life. This increase may suggest that the rate of agmatine elimination after oral administration is limited by the rate of absorption. This change in rate limitation is a characteristic of "flip-flop" kinetics, in which the rate of elimination seen in concentration-time profiles better represents the rate of absorption. Numerous factors can drive this "flip-flop," including high P-glycoprotein (P-gp) substrate activity, fast elimination in plasma, and limited permeability across biologic membranes. Agmatine remains positively charged at physiologic pH, limiting passive transport as a major absorption mechanism. Furthermore, studies of other cationic drugs suggest that there may be negligible expression of cation transporters at the basolateral membrane of the intestinal epithelium, limiting active transport

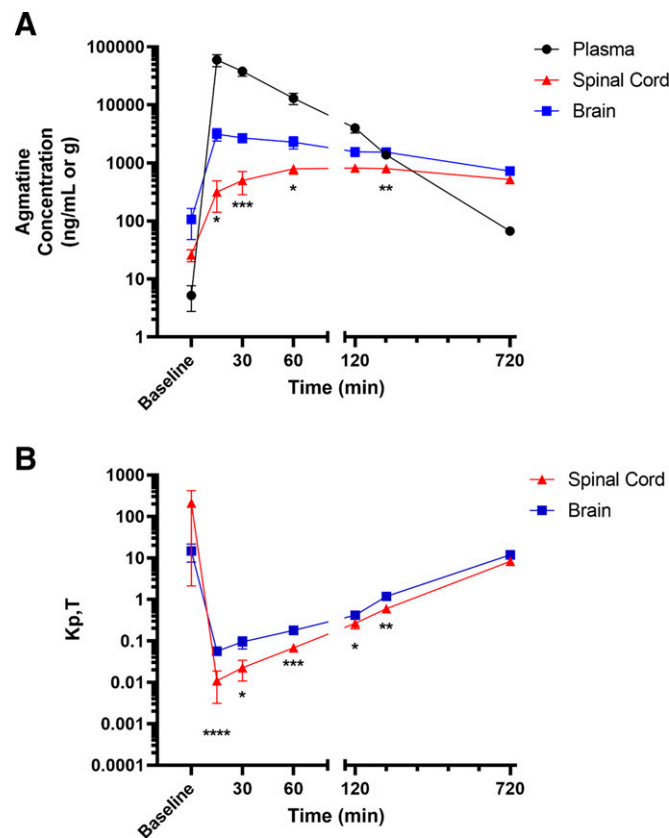


Fig. 3. Distribution of agmatine to CNS regions after intravenous administration. (A) Concentration-time profiles after a single i.v. dose of 100 mg/kg agmatine sulfate via tail-vein injection in Sprague-Dawley rat ($n = 6$). (B) Tissue-to-plasma concentration ratio over time in spinal cord and brain. Data are presented as mean \pm S.E.M.

TABLE 6

Summary of pharmacokinetic parameters of agmatine in brain and spinal cord

Summary of pharmacokinetics parameters of agmatine intravenous administration in Sprague-Dawley rat plasma, spinal cord, and brain. Results are presented as pharmacokinetic parameters determined via sparse sampling.

	Plasma	Spinal Cord	Brain
$t_{1/2}$ (min)	104	857	510
CL (ml/min/kg)	26.2	—	—
V (l/kg)	3.92	—	—
t_{max} (min)	15	120	15
C_{max} (ng/ml or g)	59,278	814	3138
AUC _{0-∞} (ng*hour/ml or g)	63,658	18,718	25,246
K_p	—	0.291	0.397

in the gut (Proctor et al., 2016). Although elimination half-life, clearance, and volume of distribution increased upon oral administration, clearance is similar on correction for bioavailability. This similarity is dependent on clearance calculation relying on $AUC_{0-\infty}$. In contrast, parameters that were dependent on the rate of disappearance, such as half-life and volume of distribution, maintained their difference, further supporting the hypothesized “flip-flop” kinetics.

Agmatine is known to cross the BBB (Piletz et al., 2003), but the extent of absorption over time as well as variation between brain and spinal cord are incompletely understood. In this study, we determined a concentration-time profile for agmatine in plasma, brain, and spinal cord in rat after intravenous administration using a terminal sampling method. In plasma, elimination half-life was greater and clearance was lower than these parameters compared with the serial sampling systemic studies. This change may be due to an increase in intravenous dose (100 mg/kg for terminal sampling, 30 mg/kg for serial sampling), potentially saturating elimination and distribution mechanisms, but no prior dose-dependence has been observed. Another source of variability is the age and weight of the animals studied. Catheterized animals for serial sampling were consistently older and heavier than the animals used for terminal sampling. Sprague-Dawley rats have been shown to have altered levels of agmatine and arginine metabolic pathways in the brain at various ages (Liu et al., 2008; Gupta et al., 2012; Jing et al., 2016). In addition, age- and weight-related changes in fat content and renal function may further alter the pharmacokinetic parameters. Furthermore, absolute concentrations may vary due to differences in collection via jugular vein (serial sampling) and trunk blood (terminal sampling).

After 100 mg/kg i.v. agmatine sulfate administration, brain distribution of agmatine is rapid ($t_{max} = 15$ minutes). However, spinal cord distribution is delayed ($t_{max} = 120$ minutes). In addition, brain concentrations were significantly greater than spinal cord concentrations from 15 to 240 minutes. These results were surprising, as the BBB is considered to be more exclusive than the blood–spinal cord barrier (BSCB) (Wilhelm et al., 2016). However, some drugs, such as peposertib, have shown a similar lower distribution to the spinal cord (Talele et al., 2022). These reductions may be due to variability in transporter expression or different free fraction within the tissue. Prior evidence supports the involvement of multidrug and toxin extrusion protein 1 (MATE1) and organic cation transporter 2 (OCT2) in the uptake mechanism of agmatine (Winter et al., 2011), but differences in expression between spinal cord and brain are unknown. OCT2 has been shown to be expressed in cultured brain microvessel endothelial cells (Lin et al., 2010), and both OCT2 and MATE1 show high expression in the leptomeninges of rats (Huttunen et al., 2022). This expression allows for possible distribution from the CSF to the spinal or brain tissue, but the density of CNS parenchyma severely limits the depth to which drugs can diffuse (Pardridge, 2011). The efflux transporters P-gp and breast cancer resistance protein (BCRP), critical components to maintain BBB and BSCB integrity, are shown to have lower expression in spinal cord capillaries compared with cortical capillaries, although studies in P-gp–null mice suggest equivalent function across these tissues (Campos et al., 2012; Uchida et al., 2020). Additionally, although variability in tissue binding may explain differences in partition coefficients between brain and spinal cord, this factor will have no impact on the rate of

distribution. Therefore, the active transport mechanism of agmatine across the BBB and BSCB may be fundamentally distinct, potentially due to different extent of involvement of the known or unknown transporters.

Once distribution of agmatine to the CNS occurred, the rate of elimination was much slower than seen in plasma. The elimination half-lives were 8.5 hours (brain) and 14.3 hours (spinal cord) compared with 104 minutes (plasma). The elimination half-life in CNS is similar to that reported for spinal cord in mouse (Roberts et al., 2005). This shorter half-life in plasma leads to greater CNS concentrations over plasma concentrations at 12 hours postdose, represented by a shift in partition coefficient to be greater than one. Notably, this CNS distribution persists long past acute activity of agmatine in pain-related behavioral assays in rat (Horváth et al., 1999; Karadag et al., 2003; Önal et al., 2003). Agmatine is known to be taken up into spinal nerve terminals, suggesting that sequestration may prevent prolonged activity (Goracke-Postle et al., 2007b).

To completely characterize the action of agmatine, both as a pharmacological agent and an endogenous neuromodulator, characterization of its distribution within the CNS is critical. The analytical method presented here has allowed deeper insight into the distributional patterns of agmatine across several biologic barriers. Furthermore, these results suggest that agmatine experiences different conditions when accessing either brain or spinal cord. This distinction has not been extensively detailed and could serve as a functional explanation for variability across spinal and cerebral responses.

Data Availability

The data that support the findings of this study are available upon request from the corresponding author.

Authorship Contributions

Participated in research design: Clements, Peterson, Wilcox, Fairbanks.

Conducted experiments: Clements, Peterson, Kitto, Caye.

Performed data analysis: Clements.

Wrote or contributed to the writing of the manuscript: Clements, Caye, Wilcox, Fairbanks.

References

- Baldini A, Von Korff M, and Lin EH (2012) A review of potential adverse effects of long-term opioid therapy: a practitioner's guide. *Prim Care Companion CNS Disord* 14:PCC.11m01326.
- Barron S, Mulholland PJ, Littleton JM, and Prendergast MA (2008) Age and gender differences in response to neonatal ethanol withdrawal and polyamine challenge in organotypic hippocampal cultures. *Alcohol Clin Exp Res* 32:929–936.
- Bergin DH, Jing Y, Williams G, Mockett BG, Zhang H, Abraham WC, and Liu P (2019) Safety and neurochemical profiles of acute and sub-chronic oral treatment with agmatine sulfate. *Sci Rep* 9:12669.
- Campos CR, Schröter C, Wang X, and Miller DS (2012) ABC transporter function and regulation at the blood-spinal cord barrier. *J Cereb Blood Flow Metab* 32:1559–1566.
- Courteix C, Privat AM, Péliissier T, Hernandez A, Eschalier A, and Fialip J (2007) Agmatine induces antihyperalgesic effects in diabetic rats and a superadditive interaction with R(-)-3-(2-carboxypiperazine-4-yl)-propyl-1-phosphonic acid, a N-methyl-D-aspartate-receptor antagonist. *J Pharmacol Exp Ther* 322:1237–1245.
- Dahlhamer J, Lucas J, Zelaya C, Nahin R, Mackey S, DeBar L, Kerns R, Von Korff M, Porter L, and Helmick C (2018) Prevalence of chronic pain and high-impact chronic pain among adults - United States, 2016. *MMWR Morb Mortal Wkly Rep* 67:1001–1006.
- Dalluge JJ, McCurtain JL, Gilbertsen AJ, Kalstabakken KA, and Williams BJ (2015) Determination of agmatine using isotope dilution UPLC-tandem mass spectrometry: application to the characterization of the arginine decarboxylase pathway in *Pseudomonas aeruginosa*. *Anal Bioanal Chem* 407:5513–5519.
- Donertas B, Cengelli Unel C, Aydin S, Ulupinar E, Ozatik O, Kaygisiz B, Yildirim E, and Erol K (2018) Agmatine co-treatment attenuates allodynia and structural

- abnormalities in cisplatin-induced neuropathy in rats. *Fundam Clin Pharmacol* **32**:288–296.
- Fairbanks CA, Schreiber KL, Brewer KL, Yu CG, Stone LS, Kitto KF, Nguyen HO, Grocholski BM, Shoeman DW, Kehl LJ, et al. (2000) Agmatine reverses pain induced by inflammation, neuropathy, and spinal cord injury. *Proc Natl Acad Sci USA* **97**:10584–10589.
- Feroli ME, Pinotti O, and Pirona L (1999) Gender-related differences in polyamine oxidase activity in rat tissues. *Amino Acids* **17**:139–148.
- Gibson DA, Harris BR, Rogers DT, and Littleton JM (2002) Radioligand binding studies reveal agmatine is a more selective antagonist for a polyamine-site on the NMDA receptor than arcaïne or ifenprodil. *Brain Res* **952**:71–77.
- Goracke-Postle CJ, Nguyen HO, Stone LS, and Fairbanks CA (2006) Release of tritiated agmatine from spinal synaptosomes. *Neuroreport* **17**:13–17.
- Goracke-Postle CJ, Overland AC, Riedl MS, Stone LS, and Fairbanks CA (2007a) Potassium- and capsaicin-induced release of agmatine from spinal nerve terminals. *J Neurochem* **102**:1738–1748.
- Goracke-Postle CJ, Overland AC, Stone LS, and Fairbanks CA (2007b) Agmatine transport into spinal nerve terminals is modulated by polyamine analogs. *J Neurochem* **100**:132–141.
- Gupta N, Jing Y, Collie ND, Zhang H, and Liu P (2012) Ageing alters behavioural function and brain arginine metabolism in male Sprague-Dawley rats. *Neuroscience* **226**:178–196.
- Horváth G, Kékesi G, Dobos I, Szikszay M, Klimscha W, and Benedek G (1999) Effect of intrathecal agmatine on inflammation-induced thermal hyperalgesia in rats. *Eur J Pharmacol* **368**:197–204.
- Huttunen KM, Terasaki T, Urtti A, Montaser AB, and Uchida Y (2022) Pharmacoproteomics of brain barrier transporters and substrate design for the brain targeted drug delivery. *Pharm Res* **39**:1363–1392.
- Jing Y, Liu P, and Leitch B (2016) Region-specific changes in presynaptic agmatine and glutamate levels in the aged rat brain. *Neuroscience* **312**:10–18.
- Karadag HC, Ulugol A, Tamer M, Ipci Y, and Dokmeci I (2003) Systemic agmatine attenuates tactile allodynia in two experimental neuropathic pain models in rats. *Neurosci Lett* **339**:88–90.
- Keynan O, Mirovsky Y, Dekel S, Gilad VH, and Gilad GM (2010) Safety and efficacy of dietary agmatine sulfate in lumbar disc-associated radiculopathy. An open-label, dose-escalating study followed by a randomized, double-blind, placebo-controlled trial. *Pain Med* **11**:356–368.
- Kolesnikov Y, Jain S, and Pasternak GW (1996) Modulation of opioid analgesia by agmatine. *Eur J Pharmacol* **296**:17–22.
- Lin CJ, Tai Y, Huang MT, Tsai YF, Hsu HJ, Tzen KY, and Liou HH (2010) Cellular localization of the organic cation transporters, OCT1 and OCT2, in brain microvessel endothelial cells and its implication for MPTP transport across the blood-brain barrier and MPTP-induced dopaminergic toxicity in rodents. *J Neurochem* **114**:717–727.
- Liu P, Chary S, Devaraj R, Jing Y, Darlington CL, Smith PF, Tucker IG, and Zhang H (2008) Effects of aging on agmatine levels in memory-associated brain structures. *Hippocampus* **18**:853–856.
- Molderings GJ, Heinen A, Menzel S, Lübbecke F, Homann J, and Göthert M (2003) Gastrointestinal uptake of agmatine: distribution in tissues and organs and pathophysiological relevance. *Ann N Y Acad Sci* **1009**:44–51.
- Morgan AD, Campbell UC, Fons RD, and Carroll ME (2002) Effects of agmatine on the escalation of intravenous cocaine and fentanyl self-administration in rats. *Pharmacol Biochem Behav* **72**:873–880.
- Nguyen HO, Goracke-Postle CJ, Kaminski LL, Overland AC, Morgan AD, and Fairbanks CA (2003) Neuropharmacokinetic and dynamic studies of agmatine (decarboxylated arginine). *Ann N Y Acad Sci* **1009**:82–105.
- Ónal A, Delen Y, Ülker S, and Soykan N (2003) Agmatine attenuates neuropathic pain in rats: possible mediation of nitric oxide and noradrenergic activity in the brainstem and cerebellum. *Life Sci* **73**:413–428.
- Osborne NR and Davis KD (2022) Sex and gender differences in pain. *Int Rev Neurobiol* **164**:277–307.
- Pardridge WM (2011) Drug transport in brain via the cerebrospinal fluid. *Fluids Barriers CNS* **8**:7.
- Peterson CD, Kitto KF, Verma H, Pflipsen K, Delpire E, Wilcox GL, and Fairbanks CA (2021) Agmatine requires GluN2B-containing NMDA receptors to inhibit the development of neuropathic pain. *Mol Pain* **17**:17448069211029171.
- Piletz JE, May PJ, Wang G, and Zhu H (2003) Agmatine crosses the blood-brain barrier. *Ann N Y Acad Sci* **1009**:64–74.
- Proctor WR, Ming X, Bourdet D, Han TK, Everett RS, and Thakker DR (2016) Why does the intestine lack basolateral efflux transporters for cationic compounds? A provocative hypothesis. *J Pharm Sci* **105**:484–496.
- Raasch W, Schäfer U, Qadri F, and Dominiak P (2002) Agmatine, an endogenous ligand at imidazole binding sites, does not antagonize the clonidine-mediated blood pressure reaction. *Br J Pharmacol* **135**:663–672.
- Reis DJ and Regunathan S (1998) Agmatine: a novel neurotransmitter? *Adv Pharmacol* **42**:645–649.
- Roberts JC, Grocholski BM, Kitto KF, and Fairbanks CA (2005) Pharmacodynamic and pharmacokinetic studies of agmatine after spinal administration in the mouse. *J Pharmacol Exp Ther* **314**:1226–1233.
- Rosenberg ML, Tohidi V, Sherwood K, Gayen S, Medel R, and Gilad GM (2020) Evidence for dietary agmatine sulfate effectiveness in neuropathies associated with painful small fiber neuropathy. A pilot open-label consecutive case series study. *Nutrients* **12**:576.
- Su RB, Wang WP, Lu XQ, Wu N, Liu ZM, and Li J (2009) Agmatine blocks acquisition and re-acquisition of intravenous morphine self-administration in rats. *Pharmacol Biochem Behav* **92**:676–682.
- Talele S, Zhang W, Oh JH, Burgenske DM, Mladek AC, Dragojevic S, Sarkaria JN, and Elmquist WF (2022) Central nervous system delivery of the catalytic subunit of DNA-dependent protein kinase inhibitor peposertib as radiosensitizer for brain metastases. *J Pharmacol Exp Ther* **381**:217–228.
- Uchida Y, Yagi Y, Takao M, Tano M, Umetsu M, Hirano S, Usui T, Tachikawa M, and Terasaki T (2020) Comparison of absolute protein abundances of transporters and receptors among blood-brain barriers at different cerebral regions and the blood-spinal cord barrier in humans and rats. *Mol Pharm* **17**:2006–2020.
- Waataja JJ, Peterson CD, Verma H, Goracke-Postle CJ, Séguéla P, Delpire E, Wilcox GL, and Fairbanks CA (2019) Agmatine preferentially antagonizes GluN2B-containing N-methyl-D-aspartate receptors in spinal cord. *J Neurophysiol* **121**:662–671.
- Wade CL, Schuster DJ, Domingo KM, Kitto KF, and Fairbanks CA (2008) Supraspinally-administered agmatine attenuates the development of oral fentanyl self-administration. *Eur J Pharmacol* **587**:135–140.
- Wang X, Ying W, Dunlap KA, Lin G, Satterfield MC, Burghardt RC, Wu G, and Bazer FW (2014) Arginine decarboxylase and agmatinase: an alternative pathway for de novo biosynthesis of polyamines for development of mammalian conceptuses. *Biol Reprod* **90**:84.
- Wilhelm I, Nyúl-Tóth Á, Suciú M, Hermenean A, and Krizbai IA (2016) Heterogeneity of the blood-brain barrier. *Tissue Barriers* **4**:e1143544.
- Winter TN, Elmquist WF, and Fairbanks CA (2011) OCT2 and MATE1 provide bidirectional agmatine transport. *Mol Pharm* **8**:133–142.
- Zelaya CE, Dahlhamer JM, Lucas JW, and Connor EM (2020) Chronic pain and high-impact chronic pain among U.S. adults, 2019. *NCHS Data Brief* **2020**:1–8.
- Zhao S, Feng Y, LeBlanc MH, Piletz JE, and Liu Y-M (2002) Quantitation of agmatine by liquid chromatography with laser-induced fluorescence detection. *Anal Chim Acta* **470**:155–161 DOI: 10.1016/S0003-2670(02)00777-8.

Address correspondence to: Dr. Carolyn A. Fairbanks, University of Minnesota, 9-177 Weaver-Densford Hall, 308 Harvard Street SE, Minneapolis, MN 55455. E-mail: carfair@umn.edu
